Exercise 6.22 Show that $\hat{E}(\boldsymbol{\kappa})$ (Eq. 6.158) is real, non-negative, with

$$\hat{E}(\boldsymbol{\kappa}) = \hat{E}(-\boldsymbol{\kappa}). \tag{6.175}$$

Exercise 6.23 Starting from the spectral representation for $\mathbf{u}(\mathbf{x})$ (Eq. 6.119), show that the spectral representation of $\partial u_i/\partial x_k$ is

$$\frac{\partial u_i}{\partial x_k} = \sum_{\boldsymbol{\kappa}} i\kappa_k \hat{u}_i(\boldsymbol{\kappa}) e^{i\boldsymbol{\kappa}\cdot\mathbf{x}}. \tag{6.176}$$

Hence show the relations

$$\begin{aligned} \left\langle \frac{\partial u_i}{\partial x_k} \frac{\partial u_j}{\partial x_\ell} \right\rangle &= \sum_{\boldsymbol{\kappa}} \kappa_k \kappa_\ell \hat{R}_{ij}(\boldsymbol{\kappa}) \\ &= \iiint_{-\infty}^{\infty} \bar{\kappa}_k \bar{\kappa}_\ell \Phi_{ij}(\bar{\boldsymbol{\kappa}})\, \mathrm{d}\bar{\boldsymbol{\kappa}}, \end{aligned} \tag{6.177}$$

and

$$\begin{aligned} \varepsilon &= \sum_{\boldsymbol{\kappa}} 2\nu\kappa^2 \hat{E}(\boldsymbol{\kappa}) \\ &= \iiint_{-\infty}^{\infty} 2\nu\bar{\kappa}^2 \tfrac{1}{2}\Phi_{ii}(\bar{\boldsymbol{\kappa}})\, \mathrm{d}\bar{\boldsymbol{\kappa}}. \end{aligned} \tag{6.178}$$

6.5 Velocity Spectra

In the previous section, the velocity spectrum tensor $\Phi_{ij}(\boldsymbol{\kappa}, t)$ is defined (for homogeneous turbulence) as the Fourier transform of the two-point velocity correlation $R_{ij}(\mathbf{r})$. (We now use $\boldsymbol{\kappa}$ for the continuous wavenumber variable, in place of $\bar{\boldsymbol{\kappa}}$ used above.) In Section 6.5.1 the properties of $\Phi_{ij}(\boldsymbol{\kappa}, t)$ are reviewed and related quantities are introduced, primarily, the energy spectrum function $E(\kappa, t)$ and the one-dimensional spectra $E_{ij}(\kappa_1, t)$. The Kolmogorov hypotheses have implications for the forms of these spectra at high wavenumber (i.e., in the universal equilibrium range). These implications are presented in Section 6.5.2, and experimentally measured spectra are presented as further tests of the hypotheses. Section 6.6 describes the energy cascade in wavenumber space in terms of the energy spectrum function $E(\kappa, t)$.

6.5.1 Definitions and Properties

Velocity Spectrum Tensor. In homogeneous turbulence, the two-point velocity correlation and the velocity spectrum tensor form a Fourier transform pair:

$$\Phi_{ij}(\boldsymbol{\kappa}) = \frac{1}{(2\pi)^3} \iiint_{-\infty}^{\infty} R_{ij}(\mathbf{r}) e^{-i\boldsymbol{\kappa}\cdot\mathbf{r}} \, \mathrm{d}\mathbf{r}, \tag{6.179}$$

$$R_{ij}(\mathbf{r}) = \iiint_{-\infty}^{\infty} \Phi_{ij}(\boldsymbol{\kappa}) e^{i\boldsymbol{\kappa}\cdot\mathbf{r}} \, \mathrm{d}\boldsymbol{\kappa}. \tag{6.180}$$

Here $\boldsymbol{\kappa} = \{\kappa_1, \kappa_2, \kappa_3\}$ is the (continuous) wavenumber vector; and, to abbreviate the notation, the dependence of R_{ij} and Φ_{ij} on time is not shown explicitly. The velocity spectrum tensor $\Phi_{ij}(\boldsymbol{\kappa})$ is a complex quantity which has the properties

$$\Phi_{ij}(\boldsymbol{\kappa}) = \Phi^*_{ji}(\boldsymbol{\kappa}) = \Phi_{ji}(-\boldsymbol{\kappa}), \tag{6.181}$$

and

$$\kappa_i \Phi_{ij}(\boldsymbol{\kappa}) = \kappa_j \Phi_{ij}(\boldsymbol{\kappa}) = 0. \tag{6.182}$$

Equation (6.181) stems from the symmetry properties of $R_{ij}(\mathbf{r})$ and from the fact that $R_{ij}(\mathbf{r})$ is real; while Eq. (6.182) is a result of incompressibility (see Exercise 6.20). In addition $\Phi_{ij}(\boldsymbol{\kappa})$ is positive semi-definite, i.e.,

$$\Phi_{ij}(\boldsymbol{\kappa}) Y_i Y_j \geq 0, \tag{6.183}$$

for all vectors $\mathbf{Y}$ (see Exercise 6.21). It then follows that the diagonal components of $\Phi_{ij}(\boldsymbol{\kappa})$ (i.e., $i = j$) are real and non-negative, and therefore so also is the trace:

$$\Phi_{ii}(\boldsymbol{\kappa}) = \Phi^*_{ii}(\boldsymbol{\kappa}) \geq 0. \tag{6.184}$$

The velocity spectrum tensor $\Phi_{ij}(\boldsymbol{\kappa})$ is a useful quantity to consider because (as shown in Section 6.4.3) it represents the *Reynolds stress density* in wavenumber space: that is, $\Phi_{ij}(\boldsymbol{\kappa})$ is the contribution (per unit volume in wavenumber space) from the Fourier mode $e^{i\boldsymbol{\kappa}\cdot\mathbf{x}}$ to the Reynolds stress $\langle u_i u_j \rangle$. In particular, setting $\mathbf{r} = 0$ in Eq. (6.180) we obtain

$$R_{ij}(0) = \langle u_i u_j \rangle = \iiint_{-\infty}^{\infty} \Phi_{ij}(\boldsymbol{\kappa}) \, \mathrm{d}\boldsymbol{\kappa}. \tag{6.185}$$

(Note that Φ_{ij} has dimensions of (velocity)^2/(wavenumber)^3, or equivalently (velocity)$^2\times$ (length)^3.)

The information contained in $\Phi_{ij}(\boldsymbol{\kappa})$ can be considered in three parts. First, the subscripts (i and j) give the directions of the velocity in physical space. So, for example, $\Phi_{22}(\boldsymbol{\kappa})$ pertains entirely to the field $u_2(\mathbf{x})$. Second, the wavenumber direction $\boldsymbol{\kappa}/|\boldsymbol{\kappa}|$ gives the direction in physical space of the Fourier mode. And third, the wavenumber magnitude determines the lengthscale of the mode, i.e., $\ell = 2\pi/|\boldsymbol{\kappa}|$ (see Fig. 6.8).

Velocity derivative information is also contained in $\Phi_{ij}(\boldsymbol{\kappa})$, in particular,

$$\left\langle \frac{\partial u_i}{\partial x_k}\frac{\partial u_j}{\partial x_\ell}\right\rangle = \int_{-\infty}^{\infty}\!\!\int\!\!\int \kappa_k\kappa_\ell\Phi_{ij}(\boldsymbol{\kappa})\,\mathrm{d}\boldsymbol{\kappa}, \tag{6.186}$$

so that the dissipation rate is

$$\varepsilon = \int_{-\infty}^{\infty}\!\!\int\!\!\int 2\nu\kappa^2\tfrac{1}{2}\Phi_{ii}(\boldsymbol{\kappa})\,\mathrm{d}\boldsymbol{\kappa}, \tag{6.187}$$

(see Exercise 6.23).

The relationship between $\Phi_{ij}(\boldsymbol{\kappa})$ and the integral lengthscales is given below (Eqs. 6.210 and 6.213).

Energy Spectrum Function. Being a second-order tensor function of a vector, $\Phi_{ij}(\boldsymbol{\kappa})$ contains a great deal of information. A simpler though less complete description is provided by the energy spectrum function $E(\kappa)$, which is a scalar function of a scalar.

The energy spectrum function is obtained from $\Phi_{ij}(\boldsymbol{\kappa})$ by removing all directional information. The information about the direction of the velocities is removed by considering (half) the trace, i.e., $\frac{1}{2}\Phi_{ii}(\boldsymbol{\kappa})$. The information about the direction of the Fourier modes is removed by integrating over all wavenumbers $\boldsymbol{\kappa}$ of magnitude $|\boldsymbol{\kappa}| = \kappa$. To express this mathematically, we denote by $\mathcal{S}(\kappa)$ the sphere in wavenumber space, centered at the origin, with radius κ; and integration over the surface of this sphere is denoted by $\oint(\quad)\,\mathrm{d}\mathcal{S}(\kappa)$. Thus the energy spectrum function is defined as

$$E(\kappa) = \oint \tfrac{1}{2}\Phi_{ii}(\boldsymbol{\kappa})\,\mathrm{d}\mathcal{S}(\kappa). \tag{6.188}$$

Alternatively, on account of the sifting property of the Dirac delta function (see Eq. C.11), an equivalent expression is

$$E(\kappa) = \int\!\!\int\!\!\int_{-\infty}^{\infty} \tfrac{1}{2}\Phi_{ii}(\boldsymbol{\kappa})\delta(|\boldsymbol{\kappa}| - \kappa)\,\mathrm{d}\boldsymbol{\kappa}, \tag{6.189}$$

where κ is here an independent variable (i.e., independent of $\boldsymbol{\kappa}$).

The properties of $E(\kappa)$ follow straightforwardly from those of $\Phi_{ij}(\boldsymbol{\kappa})$: $E(\kappa)$ is real, non-negative, and for negative κ it is undefined according to Eq. (6.188), or zero according to Eq. (6.189). Integration of $E(\kappa)$ over all κ is the same as integration of $\frac{1}{2}\Phi_{ii}(\boldsymbol{\kappa})$ over all $\boldsymbol{\kappa}$. Thus from Eqs. (6.185) and Eqs. (6.187) we obtain for the turbulent kinetic energy

$$k = \int_0^\infty E(\kappa)\,\mathrm{d}\kappa, \tag{6.190}$$

and for the dissipation

$$\varepsilon = \int_0^\infty 2\nu\kappa^2 E(\kappa)\,\mathrm{d}\kappa. \tag{6.191}$$

Evidently, $E(\kappa)\,\mathrm{d}\kappa$ is the contribution to k from all wavenumbers $\boldsymbol{\kappa}$ in the infinitesimal shell $\kappa \le |\boldsymbol{\kappa}| < \kappa + \mathrm{d}\kappa$ in wavenumber space.

In general, $\Phi_{ij}(\boldsymbol{\kappa})$ contains much more information than $E(\kappa)$: but in isotropic turbulence $\Phi_{ij}(\boldsymbol{\kappa})$ is completely determined by $E(\kappa)$. If the turbulence is isotropic, the directional information in $\Phi_{ij}(\boldsymbol{\kappa})$ can depend only on $\boldsymbol{\kappa}$, and, to within scalar multiples, the only second-order tensors that can be formed from $\boldsymbol{\kappa}$ are δ_{ij} and $\kappa_i\kappa_j$. Consequently, in isotropic turbulence, $\Phi_{ij}(\boldsymbol{\kappa})$ is given by

$$\Phi_{ij}(\boldsymbol{\kappa}) = A(\kappa)\delta_{ij} + B(\kappa)\kappa_i\kappa_j, \tag{6.192}$$

where $A(\kappa)$ and $B(\kappa)$ are scalar functions of κ. These scalar functions are readily determined (see Exercise 6.25), to yield the result that in isotropic turbulence the velocity spectrum tensor is

$$\begin{aligned}\Phi_{ij}(\boldsymbol{\kappa}) &= \frac{E(\kappa)}{4\pi\kappa^2}\left(\delta_{ij} - \frac{\kappa_i\kappa_j}{\kappa^2}\right) \\ &= \frac{E(\kappa)}{4\pi\kappa^2}P_{ij}(\boldsymbol{\kappa}),\end{aligned} \tag{6.193}$$

where $P_{ij}(\boldsymbol{\kappa})$ is the projection tensor (Eq. 6.133).

If it is assumed that $\Phi_{ij}(\boldsymbol{\kappa})$ is analytic at the origin, then $E(\kappa)$ varies as κ^4 for small κ (see Exercise 6.26). But it is possible for $\Phi_{ij}(\boldsymbol{\kappa})$ to be non-analytic, with $E(\kappa)$ varying as κ^2 (Saffman 1967) . In direct numerical simulations both κ^2 and κ^4 behaviors can be obtained (Chasnov 1995). There are suggestions (e.g., Reynolds 1987) that grid turbulence produces κ^2 behavior, but the evidence is not conclusive.

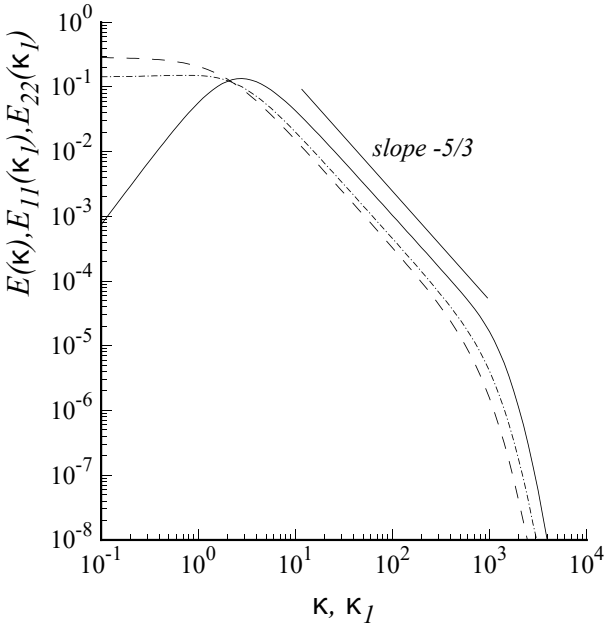

Figure 6.11: Comparison of spectra in isotropic turbulence at $R_\lambda = 500$: solid line, $E(\kappa)$; dashed line, $E_{11}(\kappa_1)$; dot-dashed line, $E_{22}(\kappa_1)$. From the model spectrum, Eq. (6.246). (Arbitrary units.)

6.5.2 Kolmogorov Spectra

According to the Kolmogorov hypotheses, in any turbulent flow at sufficiently high Reynolds number, the high-wavenumber portion of the velocity spectra adopt particular universal forms. This conclusion, and the forms of the *Kolmogorov spectra*, can be obtained via two different routes. The implications of the Kolmogorov hypotheses for the second-order velocity structure functions are given in Section 6.2 (e.g., Eqs. 6.29 and 6.30). The first route is to obtain the Kolmogorov spectra as the appropriate Fourier transforms of the structure functions. However, we follow the second route which is simpler though less rigorous: this is to apply the Kolmogorov hypotheses directly to the spectra.

Recall that (for any turbulent flow at sufficiently high Reynolds number) the Kolmogorov hypotheses apply to the velocity field on small length-scales, specifically in the universal equilibrium range defined by $\ell < \ell_{EI}$. In wavenumber space the corresponding range is $\kappa > \kappa_{EI} \equiv 2\pi/\ell_{EI}$.

According to the hypothesis of local isotropy, velocity statistics pertaining to the universal equilibrium range are isotropic. Consequently, for $\kappa > \kappa_{EI}$, the velocity spectrum tensor $\Phi_{ij}(\boldsymbol{\kappa})$ is given in terms of the energy spectrum function $E(\kappa)$ by Eq. (6.193); and the isotropic relations between

$E_{11}(\kappa_1)$, $E_{22}(\kappa_1)$ and $E(\kappa)$ apply (see Eqs. 6.214–6.218).

According to the first similarity hypothesis, velocity statistics pertaining to the universal equilibrium range have a universal form that is uniquely determined by ε and ν. Consequently, for $\kappa > \kappa_{EI}$, $E(\kappa)$ is a universal function of κ, ε and ν. Using ε and ν to non-dimensionalize κ and $E(\kappa)$, simple dimensional analysis shows that this universal relation can be written

$$\begin{aligned} E(\kappa) &= (\varepsilon\nu^5)^{\frac{1}{4}}\varphi(\kappa\eta) \\ &= u_\eta^2\eta\varphi(\kappa\eta), \end{aligned} \tag{6.233}$$

where $\varphi(\kappa\eta)$ is a universal non-dimensional function—the *Kolmogorov spectrum function*. Alternatively, if ε and κ are used to non-dimensionalize $E(\kappa)$, the relation is

$$E(\kappa) = \varepsilon^{\frac{2}{3}}\kappa^{-\frac{5}{3}}\Psi(\kappa\eta), \tag{6.234}$$

where $\Psi(\kappa\eta)$ is the *compensated Kolmogorov spectrum function*. These universal functions are related by

$$\Psi(\kappa\eta) = (\kappa\eta)^{\frac{5}{3}}\varphi(\kappa\eta), \tag{6.235}$$

and Eqs. (6.233) and (6.234) apply for $\kappa > \kappa_{EI}$, which corresponds to

$$\kappa\eta > \frac{2\pi\eta}{\ell_{EI}}. \tag{6.236}$$

The second similarity hypothesis applies to scales in the inertial subrange, i.e., $\eta \ll \ell \ll \ell_0$, or more precisely $\ell_{DI} < \ell < \ell_{EI}$. The corresponding range in wavenumber space is $\kappa_{EI} < \kappa < \kappa_{DI}$, see Fig. 6.12: or in terms of $\kappa\eta$:

$$1 \gg \kappa\eta \gg \eta/\ell_0, \tag{6.237}$$

or

$$\kappa_{DI}\eta = \frac{2\pi\eta}{\ell_{DI}} > \kappa\eta > \frac{2\pi\eta}{\ell_{EI}} = \kappa_{EI}\eta. \tag{6.238}$$

In the inertial subrange, according to the second similarity hypothesis, $E(\kappa)$ has a universal form uniquely determined by ε, independent of ν. In Eq. (6.234) for $E(\kappa)$, ν enters solely through η. Hence the hypothesis implies that as its argument $\kappa\eta$ tends to zero (i.e., $\kappa\eta \ll 1$, cf. Eq. 6.237), the function Ψ becomes independent of its argument, i.e., it tends to a constant, C. Hence the second similarity hypothesis predicts that in the inertial subrange the energy spectrum function is

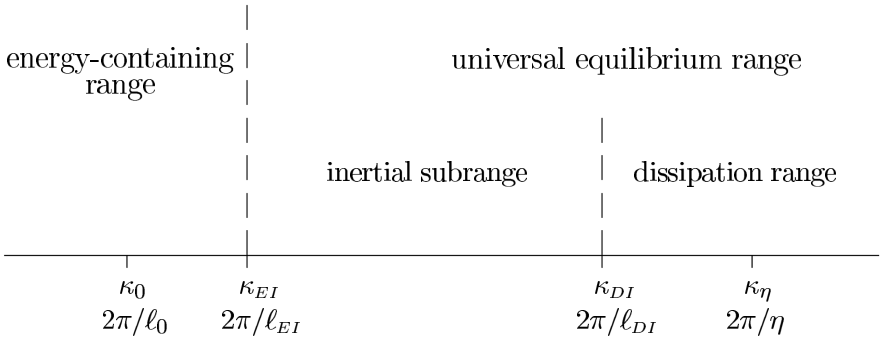

Figure 6.12: Wavenumbers (on a logarithmic scale) at very high Reynolds number showing the different ranges.

$$E(\kappa) = C\varepsilon^{\frac{2}{3}}\kappa^{-\frac{5}{3}}, \tag{6.239}$$

(i.e., Eq. 6.234 with $\Psi = C$.) This is the famous Kolmogorov $-\frac{5}{3}$ spectrum, and C is a universal Kolmogorov constant. Experimental data support the value $C = 1.5$ (see e.g., Fig. 6.17 below, and Sreenivasan 1995).

According to the hypothesis, in the inertial subrange, $\Phi_{ij}(\boldsymbol{\kappa})$ is an isotropic tensor function and $E(\kappa)$ is a power-law spectrum (i.e., Eq. 6.228 with $p = \frac{5}{3}$). Consequently, as shown in Section 6.5.1, the one-dimensional spectra are given by

$$E_{11}(\kappa_1) = C_1\varepsilon^{\frac{2}{3}}\kappa_1^{-\frac{5}{3}} \tag{6.240}$$

and

$$E_{22}(\kappa_1) = C_1'\varepsilon^{\frac{2}{3}}\kappa_1^{-\frac{5}{3}}, \tag{6.241}$$

where

$$C_1 = \tfrac{18}{55}C \approx 0.49, \tag{6.242}$$

and

$$C_1' = \tfrac{4}{3}C_1 = \tfrac{24}{55}C \approx 0.65, \tag{6.243}$$

(see Eqs. 6.228–6.232).

Some properties of power-law spectra are given in Appendix G. There is a direct correspondence between the form of $E_{11}(\kappa_1)$ (Eq. 6.240) and that of the second-order velocity structure function

$$D_{LL}(r) = C_2(\varepsilon r)^{\frac{2}{3}}, \tag{6.244}$$

Hence show that, for $C = 1.5$, the high-Reynolds-number asymptote of c_L is

$$c_L \approx (1.262\,C)^3 \approx 6.783. \tag{6.252}$$

6.5.4 Dissipation Spectra

In this and the next four subsections, experimental data, the Kolmogorov hypotheses, and the model spectrum are used to examine velocity spectra in turbulent flows. In most of the relevant experiments, Taylor's hypothesis is invoked in order to obtain measurements of the one-dimensional spectra $E_{ij}(\kappa_1)$.

Figure 6.14 is a compilation of measurements of $E_{11}(\kappa_1)$, plotted with Kolmogorov scaling. As with $E(\kappa)$ (Eq. 6.233), the Kolmogorov hypotheses imply that the scaled spectrum $\varphi_{11} \equiv E_{11}(\kappa_1)/(\varepsilon\nu^5)^{\frac{1}{4}}$ is a universal function of $\kappa_1\eta$, at sufficiently high Reynolds number, and for $\kappa_1 > \kappa_{EI}$. The data shown in Fig. 6.14 come from many different flows, with Taylor-scale Reynolds numbers from 23 to 3,180. It may be seen that for $\kappa_1\eta > 0.1$ all the data lie on a single curve. The high-Reynolds-number data ¿exhibit power-law behavior for $\kappa_1\eta < 0.1$, with the extent of the power-law region generally increasing with R_λ. Thus the data are consistent with $E_{11}(\kappa_1)/(\varepsilon\nu^5)^{\frac{1}{4}}$ being a universal function of $\kappa_1\eta$ for $\kappa_1 > \kappa_{EI}$, with the departures from universal behavior in Fig. 6.14 arising from the energy-containing range $\kappa < \kappa_{EI}$. The model spectra (also shown in Fig. 6.14 for different R_λ) appear to represent the data quite accurately.

Compensated one-dimensional spectra (i.e., $\kappa_1^{\frac{5}{3}} E_{11}(\kappa_1)$) with Kolmogorov scaling are shown in Fig. 6.15 on a linear-log plot, which emphasizes the dissipation range. For $\kappa_1\eta > 0.1$, there is close agreement between measurements in grid turbulence ($R_\lambda \approx 60$) and in a turbulent boundary layer ($R_\lambda \approx 600$), again supporting the universality of the high wavenumber spectra. The straight-line behavior evident in this plot for $\kappa_1\eta > 0.3$ corresponds to exponential decay of the spectrum at the highest wavenumbers. Again, the model spectrum represents the data accurately.

Also shown in Fig. 6.15 are the one-dimensional spectra deduced from two alternative models for $f_\eta(\kappa\eta)$. These are the exponential

$$f_\eta(\kappa\eta) = \exp(-\beta_o\kappa\eta), \tag{6.253}$$

where β_o is given by Eq. (6.258), and the *Pao spectrum*

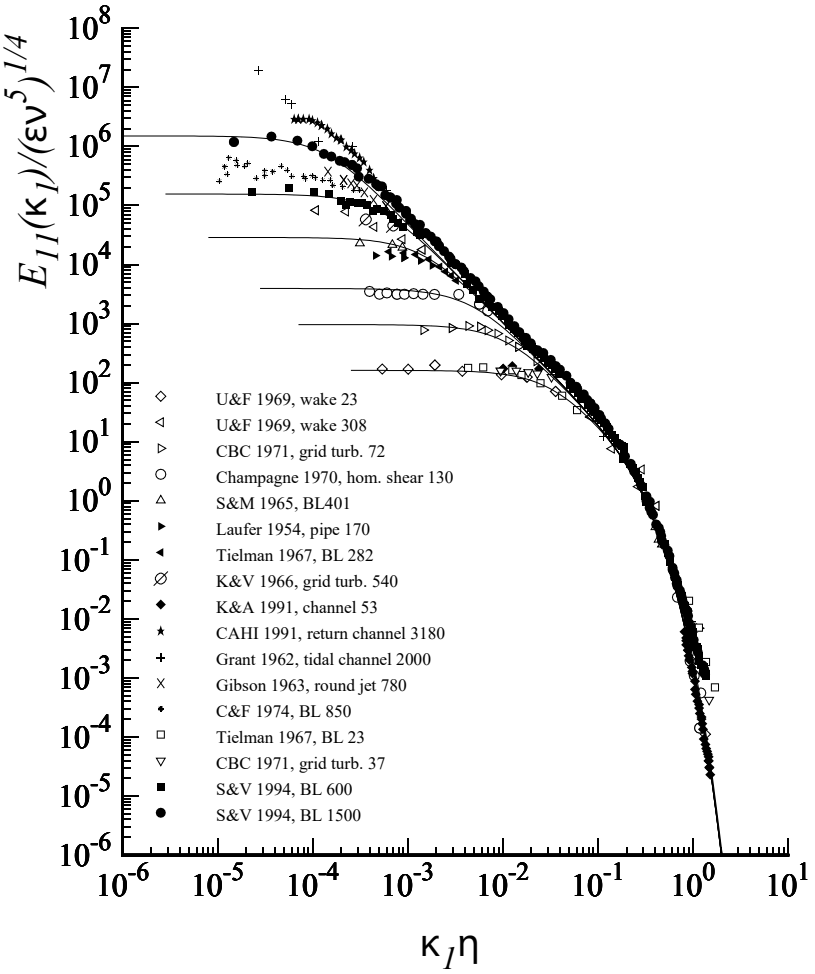

Figure 6.14: Measurements of one-dimensional longitudinal velocity spectra (symbols), and model spectra (Eq. 6.246) for $R_\lambda = 30, 70, 130, 300, 600$ and 1500 (lines). The experimental data are taken from Saddoughi and Veeravalli (1994) where references to the different experiments are given. For each experiment, the final number in the key is the value of R_λ.

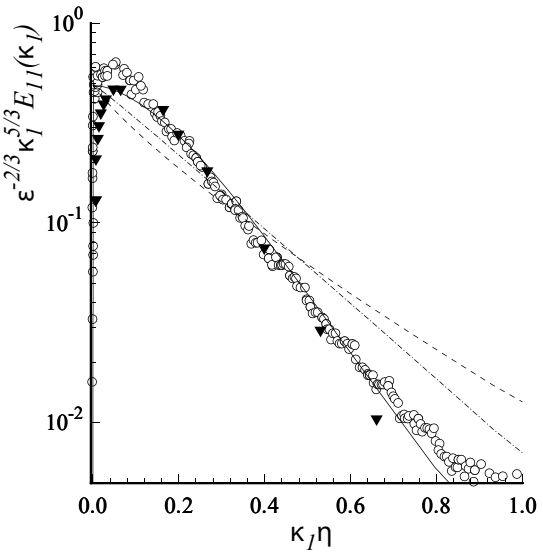

Figure 6.15: Compensated one-dimensional velocity spectra. Measurements of Comte-Bellot and Corrsin (1971) in grid turbulence at $R_\lambda \approx 60$ (triangles), and of Saddoughi and Veeravalli (1994) in a turbulent boundary layer at $R_\lambda \approx 600$ (circles). Solid line, model spectrum Eq. (6.246) for $R_\lambda = 600$; dashed line, exponential spectrum Eq. (6.253); dot-dashed line, Pao's spectrum Eq. (6.254).

$$f_\eta(\kappa\eta) = \exp(-\tfrac{3}{2}C[\kappa\eta]^{\frac{4}{3}}), \tag{6.254}$$

(see Pao 1965 and Section 6.6). It is evident from Fig. 6.15 that these alternatives do not represent the data as well as the model spectrum.

Having established that the model spectrum describes the dissipation range accurately, we now use it to quantify the scales of the dissipative motions. Figure 6.16 shows the dissipative spectrum $D(\kappa) = 2\nu\kappa^2 E(\kappa)$ according to the model for $R_\lambda = 600$, and also the cumulative dissipation

$$\varepsilon_{(0,\kappa)} \equiv \int_0^\kappa D(\kappa')\,\mathrm{d}\kappa'. \tag{6.255}$$

The abscissa shows the wavenumber κ and the corresponding wavelength $\ell = 2\pi/\kappa$, both normalized by the Kolmogorov scale η. Characteristic wavenumbers and wavelengths obtained from these curves are given in Table 6.1. It may be seen that the peak of the dissipation spectrum occurs at $\kappa\eta \approx 0.26$ corresponding to $\ell/\eta \approx 24$, while the centroid (where $\varepsilon_{(0,\kappa)} = \frac{1}{2}\varepsilon$) occurs at $\kappa\eta \approx 0.34$ corresponding to $\ell/\eta \approx 18$. Thus the motions responsible for the bulk of the dissipation ($0.1 < \kappa\eta < 0.75$, or $60 > \ell/\eta > 8$) are

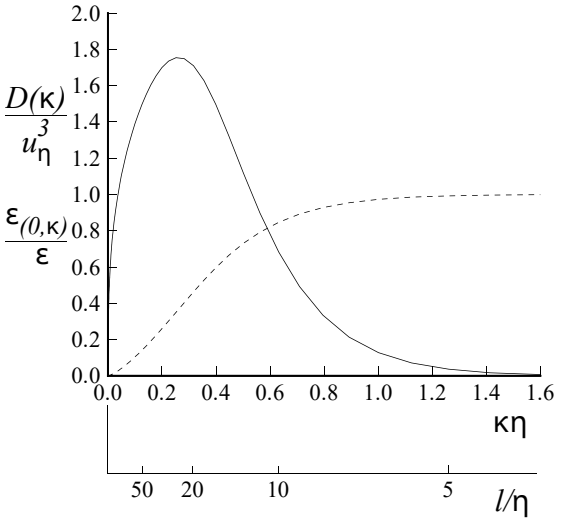

Figure 6.16: Dissipation spectrum (solid line) and cumulative dissipation (dashed line) corresponding to the model spectrum Eq. (6.246) for $R_\lambda = 600$: $\ell = 2\pi/\kappa$ is the wavelength corresponding to wavenumber κ.

considerably larger than the Kolmogorov scale. (There is no inconsistency between this observation and the Kolmogorov hypotheses: the hypotheses imply that the size of the dissipative motions *scale* with η, not that they are equal to η.) Based on these observations we take the demarcation length-scale between the inertial and dissipative ranges to be $\ell_{DI} = 60\eta$. (The significance of ℓ_{DI} is illustrated in Figs. 6.2 and 6.12.)

Exercise 6.33 Show that, at high Reynolds number, the expression for dissipation obtained from integration of the model spectrum (Eq. 6.246) is

Table 6.1: Characteristic wavenumbers and lengthscales of the dissipation spectrum. (Based on the model spectrum Eq. 6.246 at $R_\lambda = 600$.)

Defining wavenumbers	$\kappa\eta$	ℓ/η
Peak of dissipation spectrum	0.26	24
$\varepsilon_{(0,\kappa)} = 0.1\varepsilon$	0.10	63
$\varepsilon_{(0,\kappa)} = 0.5\varepsilon$	0.34	18
$\varepsilon_{(0,\kappa)} = 0.9\varepsilon$	0.73	8.6